



Rényi Entropy in Measuring Information Levels in Voronoï Tessellation Cells with Application in Digital Image Analysis

E. A-iyeh^a, James Peters^{a,b,*}

^a*Computational Intelligence Laboratory, Department of Electrical & Computer Engineering, University of Manitoba, Winnipeg, MB, R3T 5V6, Canada*

^b*Department of Mathematics, Faculty of Arts and Sciences, Adıyaman University, Adıyaman, Turkey*

Abstract

This work introduces informative and interesting Voronoï regions through measures utilizing probability density functions and qualities of Voronoï cells of digital image point patterns. Global mesh cell quality exhibits a fairly horizontal behaviour in its range of convergence across several categories of digital images. Simulation results unambiguously show that Shannon entropy does not expose the most information in Voronoï meshes although it's in the range $1 < \beta \leq 2.5$ for which information is maximized. Mesh information is seen to be generally a non-linear, non-decreasing function of image point patterns. Some important mathematical theorems on quantities and optimality conditions are proved.

Keywords: Generator, quality, Voronoï mesh, pattern, entropy, information.

2010 MSC No: Primary 54E05, Secondary 20L05, 35B36.

1. Introduction

This article introduces an approach to measuring the information levels Voronoï tessellation (mesh) cells via Rényi entropy. The focus is on the Rényi entropy of Voronoï meshes with varying quality. Let $p(x_1), \dots, p(x_i), \dots, p(x_n)$ be the probabilities of a sequence of events $x_1, \dots, x_i, \dots, x_n$ and let $\beta \geq 1$. Then the Rényi entropy (Rényi, 2011) $H_\beta(X)$ of a set of event X is defined by

$$H_\beta(X) = \frac{1}{1-\beta} \ln \sum_{i=1}^n p^\beta(x_i) \text{ (Rényi entropy).}$$

*Corresponding author: 75A Chancellor's Circle, EITC-E2-390, University of Manitoba, WPG, MB R3T 5V6, Canada; e-mail: james.peters3@ad.umanitoba.ca, research supported by Natural Sciences & Engineering Research Council of Canada (NSERC) discovery grant 185986.

Email addresses: umaiyeh@myumanitoba.ca (E. A-iyeh), James.Peters3@umanitoba.ca (James Peters)

Rényi's entropy is based on the work by R.V.L. Hartley (Hartley, 1928) and H. Nyquist (Nyquist, 1924) on the transmission of information. A proof that $H_\beta(X)$ approaches Shannon entropy as $\beta \rightarrow 1$ is given in (Bromiley et al., 2010), i.e.,

$$\lim_{\beta \rightarrow 1} \frac{1}{1-\beta} \ln \sum_{i=1}^n p^\beta(x_i) = - \sum_{i=1}^n p_i \ln p_i.$$

The information of order β contained in the observation of the event x_i with respect to the random variable X is defined by $H(X)$. In our case, it is information level of the observation of the quality of a Voronoï mesh cell viewed as random event that is considered in this study. The principle application of the proposed approach to measuring the information levels of mesh cells is the tessellation of digital images.

A main result reported in this study is the correspondence between image quality and Rényi entropy for different types of tessellated digital images. In other words, the correspondence between the Rényi entropy of mesh cells relative to the quality of the cells varies for different classes of images. For example, with Voronoï tessellations of images of humans, Rényi entropy tends to be higher for higher quality mesh cells (see, e.g., the plot in Fig. 1 for different Rényi entropy levels, ranging from $\beta = 1.5$ to 2.5 in 0.5 increments).

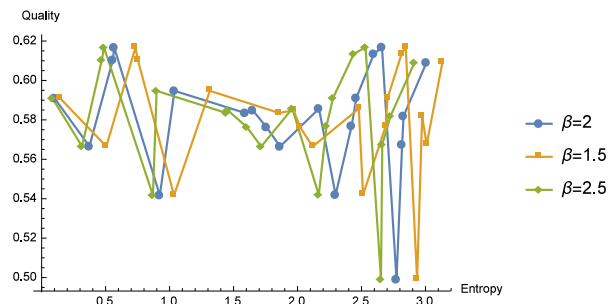


Figure 1. Rényi entropy

2. Literature Review on Voronoï Diagrams

It is known that generating meshes is a fundamental and necessary step in several domains such as engineering, computing, geometric and scientific applications (Leibon & Letscher, 2000; Owen, 1998; Liu & Liu, 2004). No matter what their domain application and the specific terminology used, the resultant meshes have structures or volumes that result from the geometry of surfaces, dimension of the space and placement or organization of generators (Ebeida & Mitchell, 2012; Mitchell, 1993; Persson, 2004). Meshes may be generated for purposes of image processing and segmentation (Arbeláez & Cohen, 2006), clustering (Ramella et al., 1998), data compression, quantization, analysis of territorial behavior of animals (Persson, 2004; Persson & Strang, 2004; Du et al., 1999) to name a few. Applications of meshes are growing but works in the direction of exploiting pattern nature and information are lacking. We are therefore of the view that understanding the pattern and the underlying process could greatly benefit applications.

Voronoï diagrams were introduced by the Ukrainian mathematician G. Voronoï (Voronoi, 1903, 1907, 1908) (elaborated in the context of proximity and quality spaces in (Peters, 2015b,c,a; A-iyeh & Peters, 2015; Peters, 2016)) provide a means of covering a space with regular polygons. The process allows us to understand fundamental properties of elements of the space by exploiting properties of the meshes. The properties of the space may otherwise have remained inaccessible.

In telecommunications, Voronoï diagrams have furnished a tool for analysis of binary linear block codes (Agrell, 1996) governing regions of block code and performance of Gaussian channels.

In musicology, Voronoï diagrams have demonstrated their utility (McLean, 2007). For example, they have been successfully applied in automatic grouping of polyphony (Hamanaka & Hirata, 2002). Other works bordering on applications of Voronoï meshes are in reservoir modeling (Møller & Skare, 2001) and cancer diagnosis (Demir & Yener, 2005).

The fact that the partitioning algorithm divides the plane into Euclidean neighborhoods permits exploitation of proximity relations while offering the flexibility of modeling the space as a continuous image-like point pattern representing the space. Given the substantial utility of Voronoï tessellations their applicability in additional areas including point pattern detection and image analysis is currently being investigated vigorously.

In this work meshes are generated for the purposes of characterizing a point pattern information using multiple measures for the individual mesh cells. The major focus here goes beyond tessellating a space with meshes. Additionally we search for important cues that may be fundamental for basic pattern understanding which in turn may lead to identifying and understanding the underlying pattern.

3. Preliminaries

In this section, the grounding theory entropy, quality of cells and Voronoï diagrams based on point pattern distributions is set. Some useful definitions are given prior to facilitate the process.

3.1. Notation and Definitions

A subset of points in \mathbb{R}^n is denoted by S . A partition of the space of $S \subseteq \mathbb{R}^n$ according to the Voronoï criterion into contiguous non-overlapping polygons is denoted by the set $\{\mathbb{V} = \mathcal{F}, \mathcal{E}, S = \mathbb{N}\}$ where \mathcal{F}, \mathcal{E} are the faces and edges of graph regions respectively. Also, properties of cells such as length of edges of polygons are represented by l_i , area by A , quality of cells by q_i and entropy by H_R .

Definition 3.1. Given a point pattern set $S \subseteq \mathbb{R}^n$ of three or more non-collinear points and a distance function d_n , the set $\{\mathbb{V}, S = \{\mathbb{N}\}$ is called a Voronoï tessellation of S if $\mathbb{V}_i \cap \mathbb{V}_j \neq \emptyset$ for $i \neq j \in S$. A Voronoï tessellation is a set of polygons with their edges and vertices that partition a given space of points.

Definition 3.2. The Voronoï region of an image point is a polygon about that site. The set of all regions partition a plane of image points based on a distance function $\|\cdot\|$. This results in a covering of the plane with polygons about the points.

Definition 3.3. Consider the set $S = \{s_1, \dots, s_k\}$, a plane (v_i, v_j) is a Voronoï edge of the Voronoï region \mathbb{V}_i if and only if there exists a point x such that the circle centered at x and circumscribing v_i and v_j does not contain in its interior any other point of \mathbb{V}_i . A Voronoï edge is a half plane equidistant from two sites and bounds some part of the Voronoï diagram. Every edge is incident upon exactly two vertices and every vertex upon at least three edges.

Definition 3.4. A Voronoï neighborhood of a point p in the vicinity of point q is the locus of bisectors or half planes equidistant from p and q . The union of half planes H_q^p (H_p^q) is the locus of points nearer to p than to q . The intersection of half planes $\bigcap_{q \in S, q \neq p} H_p^q$ defines a region generated at p .

Definition 3.5. A Voronoï vertex is the center of a circumcircle through three sites.

Definition 3.6. A set of points S is a convex set if there is a line connecting each pair of points within S .

Definition 3.7. The convex hull of Voronoï regions about S is the smallest set which contains the Voronoï regions as well as the union of the regions.

Definition 3.8. A point pattern is a set of points of the signal representing locations of signal features. For example sets of corners, keypoints etc. are referred to as point or dot patterns.

Definition 3.9. The quality of a Voronoï cell is a dimensionless real number assigned to the cell based on the extent to which the sides of the cell match.

Definition 3.10. An open pattern point is a point such that a disk centered on it contains the point as an interior point.

Definition 3.11. A closed pattern point is a point such that a disk centered on it contains the point as well a boundary.

Definition 3.12. Let \mathbb{V} be a Voronoï diagram in \mathbb{R}^2 . The skeleton of $\mathbb{V}_i \in \mathbb{V}$, is the open set $S(\Omega)$ from which the Voronoï diagram is generated.

Definition 3.13. The Voronoï quality of visual information given by a point generator is defined as the aggregate of measure of cells comprising the tessellation. In other words it shows the organization of a point pattern.

Definition 3.14. A point pattern is feasible when there exists a constant $t > 0$ such that at least one quality measure of the Voronoï cells is at least t .

3.2. Voronoï Diagrams

The spatial distribution of point sets informs the nature and organizations of the pattern. This in turn influences the graph geometry of the Voronoï diagram the point set. Assume we have a finite set S of point locations called sites s_i in a space \mathbb{R}^n . Computing the Voronoï diagram with respect to S entails partitioning the space of S into Voronoï regions $\mathbb{V}(s_i)$ in such a way that the region $\mathbb{V}(s_i)$ contains all points of S that are closer to s_i than to any other object s_j , $i \neq j$ in S .

More elaborately, given the generator set

$$S = \{s_1, \dots, s_k : i \in \mathbb{N}\},$$

the Voronoï region $\mathbb{V}(s_i)$ is defined by

$$\mathbb{V}(s_i) = \{x \in \mathbb{R}^n : \|x - s_i\| \leq \|x - s_k\|, s_k \in S, i \neq k\},$$

where $\|\cdot, \cdot\|$ is the Euclidean norm (distance between vectors). The set

$$\mathbb{V}(S) = \bigcup_{s_i \in S} \mathbb{V}(s_i)$$

is called the n -dimensional Voronoï diagram generated by the point set S . In \mathbb{R}^2 , this effectively covers the plane with convex and non overlapping graphs, one for each generating point in S . By the definition of a Voronoï region above, the region about a site x satisfies

$$d(x, s_i) \leq d(x, s_k) \Leftrightarrow \|x - s_i\|^2 \leq \|x - s_k\|^2 \forall s_i \in S.$$

Manipulating the expression of a Voronoï region gives

$$\mathbb{V}(s_i) := \{(s_k - s_i)x \leq \frac{\|s_k\|^2 - \|s_i\|^2}{2}, s_k \in S\}.$$

The immediate expression is recognized as an ordinary linear system of equations when S is finite (Goberna et al., 2012). For a partitioned space in which all the individual regions are triangles, the optimal tessellation of the point set which maximizes the minimum angle in each triangular graph is the Delaunay triangulation. The Delaunay triangulation of S is the triangulation $DT(S)$ where the circum-circles of all cells contain only the three points forming the triangle. Since a Delaunay image triangulation can be obtained from the corresponding Voronoï image graph our focus shall be on the latter. Point patterns in Delaunay image triangulations are informative and can be used to study the nature of the underlying tessellated process.

The advantage of Voronoï diagrams in studying patterns is that it associates the local neighborhood of a point with the information in the region inclosed by the point as opposed to point estimates only. Consequently measures may be aggregated for global pattern information gathering.

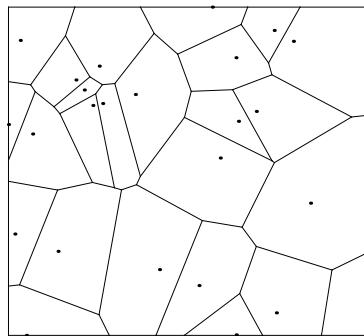


Figure 2. Voronoï mesh pattern

Fig. 3.2 displays a Voronoï diagram generated by a point set (not shown) in \mathbb{R}^2 . The diagram shows how a space partitioned into regions of influences about the generators in the form convex non-intersecting polygons. The nature of the pattern influences the distribution of the point set as well as the structure of the partitioned space. For example polygons in regions of higher point densities are of smaller sizes or areas compared to polygons of regions with lower point densities.

4. Patterns and Information Theory

Information in signals and patterns is commonly characterized using information theoretic approaches such as entropy and characteristics of a transformed space of the pattern such as quality measures of Voronoï cells. In the following subsections we present those tools.

4.1. Entropy

Entropy has long been an indicator of information and information content whose utility has since extended to other fields besides thermodynamics where it emerged. In thermodynamics, it was first used for understanding molecular structure. Entropy now finds applications in several other fields including portfolio selection and financial decision making (Zhou *et al.*, 2013), distribution analysis (Chapman, 1970) where it's founded on probability density functions derived from random variables.

Some general observations on entropic information are in order before proceeding. If all the realizations of a random variable have equal chance of being observed, then the variables have equal probabilities. Relating this to Voronoï cells this means we have a simple pattern formed by repetition of a unit. Consequently the same information is contained in all cells of the pattern. This scenario corresponds to maximization of entropy.

When a measure of information in a pattern is maximized the variations of the pattern primitives must be minimal and one variable or cell and its attribute is representative of the pattern. This situation also means there is no other information in the pattern other than the fact that the random variables of the pattern are uniformly distributed. On the contrary variations in a random variable indicates interestingness, disorder, complexity or randomness in the pattern and most importantly a distribution of variables that is anything but uniform.

4.1.1. Renyi Entropy

Renyi entropy is a general information criterion of which Shannon entropy and others are special cases (Xu & Erdogmuns, 2010). This generality is useful in diversity and dissimilarity characterization (Rao, 1982) of pattern structure. Recall that the area of a Voronoï cell satisfies $0 < A_i \leq \infty$ and so the probability $Pr(\cdot)$ of the area random variable assuming a value in the range of areas is defined in $0 \leq Pr(A_i) \leq 1$. Let A_T be the total planar surface area of a Voronoï tessellation \mathbb{V} . It follows that the probability of the random variable A_i is defined by

$$Pr(A_i) = \frac{A_i}{A_T},$$

and

$$\sum_i Pr(A_i) = 1.$$

A general entropy criterion utilizing the probability densities of the random variables is defined by:

$$H = \frac{1}{1-\beta} \ln \sum_{i=1}^n Pr_i^\beta,$$

where $Pr(A_i) = Pr_i$. A noteworthy property of Renyi entropy is majorization. Assume two finite probability vectors P and Q of length $1 < k \leq n$. P is said to majorize Q if

$$P_1 + P_2 + \cdots + P_k \geq Q_1 + Q_2 + \cdots + Q_k.$$

This means that P exhibits a stronger tendency towards uniformity than Q and thus has more entropy. This is an important indicator for understanding the nature of the distribution of a random variable.

4.2. Cell Quality

Mesh quality in the literature is sufficiently developed with guarantees for triangular and tetrahedral elements (Bern & Eppstein, 1995). However this is not so for mesh elements of four or more sides as well as hexahedra. As a result this research is necessitated in the direction of mesh elements from planar Voronoï diagrams which mostly have four or more sides towards their quality guarantees. This is where the potential utility and impact of mesh qualities in this work is directed. The quality of a mesh depicts a way of investigating pattern organization with a measure of geometric structure. The quality q of a cell is defined by the lengths of the sides of the polygon l_i and its area A . To illustrate consider a quadrilateral Voronoï cell. Its quality is defined by

$$q = 4 \frac{A}{l_1^2 + l_2^2 + l_3^2 + l_4^2}.$$

Quality factors of different kinds of polygons are adopted to the criteria of (Shewchuk, 2002; Bhatia & Lawrence, 1990; Knupp, 2001). Quality measures are defined to assume values in $0 \leq q \leq 1$. A quality value of zero corresponding to a degenerate mesh region whilst a value of one corresponds to a region with equal polygonal side lengths.

5. Theorems and Observations on Voronoï Diagrams

Let $\{q_i\}, i = 1, 2, \dots, n < \infty$ be the set of qualities of cells resulting from a Voronoï tessellation.

Theorem 5.1. *Qualities of cells satisfy the inequality*

$$(q_1 + q_2 + q_3 + \dots + q_n)^2 \leq n^2.$$

Proof. Without loss of generality assume $n = 4$. Notice that $q_i \in [0, 1]$

$$(q_1 + q_2 + q_3 + q_4)^2 = q_1^2 + 2q_1q_2 + q_2^2 + q_1q_3 + q_1q_4 + q_2q_3 + q_2q_4 + q_3^2 + 2q_3q_4 + q_4^2 + q_iq_j \leq 1.$$

Each of the individual terms is potentially less than its maximum value since all the qualities may not have $q_i = 1$. So the squared sum of the qualities is equal to n^2 if and only if all cells have a quality of 1. The quality inequality must be as it is to take care of qualities other than the extremes of zero and unity. Thus we must have

$$(q_1 + q_2 + q_3 + \dots + q_n)^2 \leq n^2,$$

for $n < \infty$. □

Theorem 5.2. For a Voronoi cell of quality $q_i = 1$ there exists a point inside the cell to which all vertices are equidistant.

Proof. See (A-iyeh & Peters, 2015). □

Theorem 5.3. For every Voronoi cell with $q = 1$ there exists a polygon whose edge lengths are not unequal.

Proof. See (A-iyeh & Peters, 2015). □

Lemma 5.1. Let $A(\mathcal{V}_s)$ be the area of the smallest polygon in a Voronoi mesh and let $A(\mathcal{V}_l)$ be the area of the polygon with the largest area in the same mesh with intermediate polygonal areas $A(\mathcal{V}_1) \dots, A(\mathcal{V}_n)$. Then

$$A(\mathcal{V}_s) \subseteq A(\mathcal{V}_l)$$

and

$$A(\mathcal{V}_s) \subseteq A(\mathcal{V}_1) \subseteq A(\mathcal{V}_2) \cdots \subseteq A(\mathcal{V}_n) \subseteq A(\mathcal{V}_l)$$

for a mesh with $n + 2$ polygons.

Lemma 5.2. The sequence of all ordered elements of the projections of sets A_1 and B_1 , i.e., $\{a_n\}$ and $\{b_n\}$, $n = 1, 2, 3, \dots$ form a metric space.

Consider polygonal elements of R^n with elements $x = (x_1, x_2, \dots, x_n)$, $y = (y_1, y_2, \dots, y_n)$. Let $\rho(A_1, B_1) = \inf\{\|x - y\| : x \in A_1, y \in B_1\}$ be the distance between functions of bounded elements A_1 and B_1 of the space. Again let $pr_n(A_1) = \inf\{x \in A_1 | \exists x_1, x_2, \dots, x_{n-1} \in R : x = (x_1, x_2, \dots, x_{n-1}) \in A_1\}$ be the projection of set A_1 onto the n^{th} -coordinate space of R^n and $\Delta_{l_1 \dots l_{n-1}}$ represents polygons (half-open meshes) of the form $(l_1 h, l_1 h + h] \times \dots \times (l_{n-1} h, l_{n-1} h + h]$. h is the edge length and l_1, l_2, \dots, l_{n-1} are integers.

Theorem 5.4. If A_1 and B_1 be bounded polygons in a Voronoi with with a function of the polygons $\rho(A_1, B_1) = \delta_0 > 0$, then a family of polygons $\{\Delta\}_{k=1}^N$, $\Delta_k \subseteq \mathbb{R}^{n-1}$ exists such that

$$pr_{\mathbb{R}^{n-1}}(A \cup B) \subseteq \prod_{i=1}^N \Delta_i,$$

for any Δ if $x \in A$, $y \in B$, $pr_{\mathbb{R}^{n-1}} x, pr_{\mathbb{R}^{n-1}} y \in \Delta_k$, then $|x_n - y_n| = |pr_n x - pr_n y| \geq \delta = \frac{\delta_0}{2}$.

Proof. Assume $h \in (0, \delta_0(2n)^{-1/2})$. Let $D_{k_1 \dots k_{n-1}} = \Delta_{k_1 \dots k_{n-1}} \mathbb{R}$. Then $D_{k_1 \dots k_{n-1}}$ possesses the following properties

1. $\bigcup_{k_1, \dots, k_{n-1} \in \mathbb{Z}} D_{k_1, \dots, k_{n-1}} = \mathbb{R}^n$
2. $D_i \cap D_j = \emptyset$
3. $\forall D = D_{k_1, \dots, k_{n-1}}$ and $\forall x, y \in D$ if $\rho(x, y) \geq \delta_0$, then $\rho(pr_n x, pr_n y) \geq \delta_0/2$

Consider $x, y \in D$ and assume $|x_n - y_n| = |pr_n x - pr_n y| < \delta_0/2$. Then we have $\rho(x, y) = [(x_1 - y_1)^2 + \dots + (x_n - y_n)^2]^{-1/2} \leq (h^2 + \dots + h^2 + \delta_0^2/4)^{-1/2}$. For $h \in (0, \delta_0(2n)^{-1/2})$, $\rho(x, y) = (\delta_0^2(n-1)/(2n) + \delta_0^2/4)^{-1/2} < \delta_0$. This is untrue. Hence, property 3 is proved.

For property 2, $A \cup B \neq \emptyset$ and the union of the bounded sets is bounded, so $\bigcup_{i=1}^N \supseteq A \cup B$. Thus the union of all the polygons covers the space \mathbb{R}^n and that proves property 1. $pr_{\mathbb{R}^{n-1}}(\bigcup_{i=1}^N D_i) = pr_{\mathbb{R}^{n-1}}(\bigcup_{k=1}^N \Delta_k \mathbb{R}) \supseteq pr_{\mathbb{R}^{n-1}}(A \cup B)$ and $\bigcup_{k=1}^N \supseteq pr_{\mathbb{R}^{n-1}}(A \cup B)$. These statements imply that for $x \in A$, $y \in B$ we can find Δ_k such that $\rho(x, y) \geq \delta_0$ by assumption, so that $\rho(pr_n x, pr_n y) = |x_n - y_n| \geq \delta_0/2 = \delta$. \square

Theorem 5.5. *Symmetry is a condition for optimality of Voronoï meshes.*

Proof. Note that \mathbb{V} for a site s can be expressed as $\mathbb{V}(s_i) := \{(s_k - s_i)x \leq \frac{\|s_k\|^2 - \|s_i\|^2}{2}, s_k \in S\}$. To show optimality we need

$$\frac{\partial \mathbb{V}(s_i)}{\partial s_i}.$$

This gives

$$\frac{\partial V(s)}{\partial s} = -x = -\frac{2\|s_i\|}{2}.$$

The immediate expression is equivalent to

$$x = \begin{cases} s_i, & \text{if } x \geq 0, \\ s_i, & \text{if } x < 0, \end{cases}$$

which is a mathematical expression for symmetry. \square

Property 1. Given a measure function $q(\cdot)$ for a Voronoï diagram of an $n \geq 3$ point set the Voronoï tessellation consists of quality functions equal in number to the number of Voronoï cells.

Property 2. The Voronoï diagram of a set S consisting of $n \geq 3$ non-collinear objects with a measure q for the polygons has at most $2n - 5$ vertices and $3n - 6$ edges, respectively.

Theorem 5.6. *The quality of a scaled Voronoï cell is scale invariant.*

Proof. Consider a triangular cell with quality $q = 1$ before scaling. Now assume the edges of the cell have been scaled with a multiplier $m > 0$. The quality before scaling is given by

$$q = 4\sqrt{3} \frac{0.5l^2}{l^2 + l^2 + l^2} = 1.$$

The quality, after scaling, is expressed by

$$q = 4\sqrt{3} \frac{0.5(ml)^2 \sqrt{\frac{3}{4}}}{(ml)^2 + (ml)^2 + (ml)^2} = 1.$$

\square

6. Applications

The utility of Voronoï tessellations has often been limited to space partitioning and not understanding the pattern as evidenced by numerous articles. Owing to this an abysmal number of works explore the potential of Voronoï diagrams beyond space partitions. Even fewer works examine properties of Voronoï cells with the viewpoint of understanding underlying nature of patterns. We attempt a way of representing part of a signal space from a point set sample distribution that summarizes the pattern by its equivalent Voronoï signature. These points in the pattern form generators for Voronoï diagrams. Keypoint image patterns of buildings, animals, humans and mountains as previously utilized in (A-iyeh & Peters, 2015) were sampled from images of dimensions M by N to summarize the signals. These point patterns consist of 50 units corresponding to the most prominent in the images. To establish a fair basis for cross analysis the same number of point sets is sampled for all images. In addition all the image signals are gray scale of their respective categories from the dataset of (Wang et al., 2001) (Fig. 4).

With the preamble in place we tessellate and cover the pattern spaces with Voronoï polygons. It is expected that since point patterns are distinct their Voronoï diagrams would exhibit discriminatory properties. This could be key in pattern discrimination using the computed quantities.

Upon identifying the subset representing an image space, we apply the Voronoï partition algorithm to the generators in the signal space. The result is a tessellated space of Voronoï polygons. Open polygons are typical of Voronoï partitions as such in the mathematical formulation of some derived features of the tessellated spaces we adopt techniques that allow the infinite polygons as well as the finite ones to be well behaved.

To help examine the nature and behaviour of patterns, plots of various quantities are given. There are as many qualities as cells so we define a global quality index or fidelity to capture the geometry of the pattern. Using all cell qualities in a tessellation it is defined by

$$q_{all} = \frac{1}{n} \sum_{i=1}^n q_i,$$

where n is the total number of cells and q_i is the quality of cell i . This enables a one-to-one correspondence between quantities.

Due to the finite nature of digital image, we limit the geometrical extent of the point patterns to their convex sets. The information content of images are assessed using a general entropy criterion. A special case of the the general entropy criterion H occurs when $\beta = 2$. This is the so called Renyi entropy denoted here H_R . Simulation results are included for $\beta = 2, 1.5, 2.5$. This range of β captures a range of entropies including the Shannon entropy at $\beta = 2$.

The choice of β in the neighborhood of 2 is not arbitrary. The reasons are two fold; on the one hand we are close to Shannon entropy which enables us to obtain information on the distribution of elements. On the other hand it gives us information on how units of a point pattern influence their distribution. Just as l_0 and l_∞ norms represent extremes of the smallest and largest elements of a set H_0 and H_∞ are the extremes of information measures of which $H_{0 < p < \infty}$ gives a tradeoff.

The simulation process is summarized in the following algorithm.

Mesh Quality(q)

for each Voronoï region $\mathbb{V}_i \in \mathbb{V}$ of S **do**

 Access the number of sides and coordinates of the vertices of the polygon.

 Using the coordinates, compute the lengths l_i and Area A of the polygon.

 Use l_i and A_i in the appropriate expression to compute its quality q_i .

end for

$Q = \{q_i\}$

Mesh Entropy(H)

for each Voronoï region $\mathbb{V}_i \in \mathbb{V}$ **do**

 Compute Pr_i

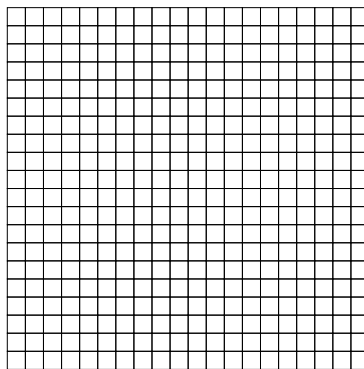
 Use Pr_i to compute H_i

$H = \{H_i\}$

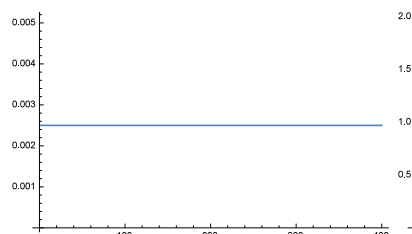
end for

Remark 6.1. The assumption made here is that the lengths of the sides of every Voronoï region polygon are measurable. Unfortunately, this is not always the case in, for example, Voronoï tessellations of 2D digital images, since some of the sides of Voronoï region polygons along the borders of an image have infinite length and border polygons have unbounded areas. To cope with this problem, the lengths of all border polygons are a measured relative to one or more image borders.

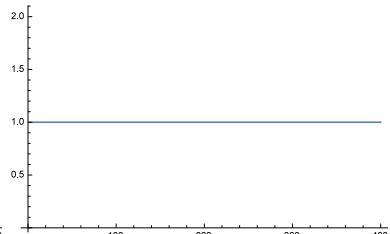
Example 1. Consider a completely regular pattern tessellated as shown in Fig. 3.



3.1: Mesh



3.2: Probability



3.3: Quality

Figure 3. Perfectly Regular Image Graph Space and Quantities

In Fig. 3 all Voronoï cells have the same area resulting in a uniform distribution of their probabilities. Also all cells have the same quality. Now there are 400 cells in the tessellation and so H attains its maximum value of 5.99146 and the global quality index also attains its maximum value of unity. From the distribution of the probability of cells and their qualities it's straight forward to see that a plot of general entropy against global quality indices would be a straight horizontal line.

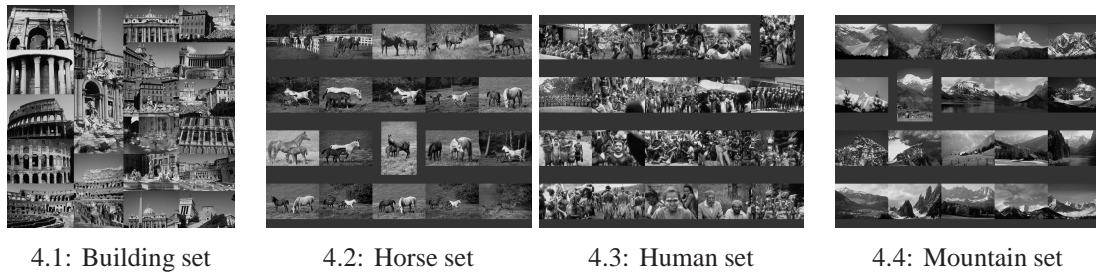


Figure 4. Data sets

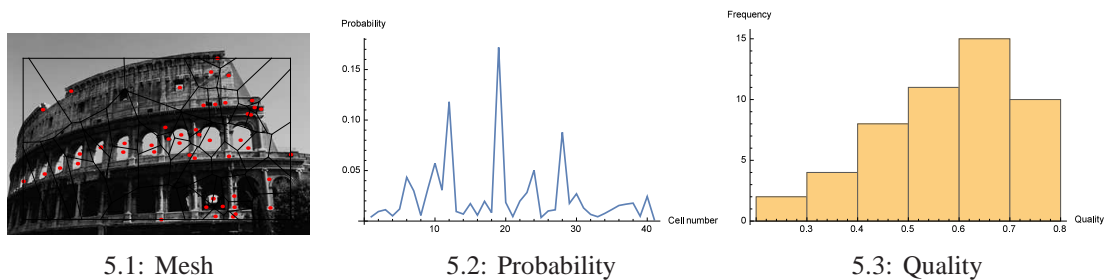


Figure 5. Image Graph Spaces

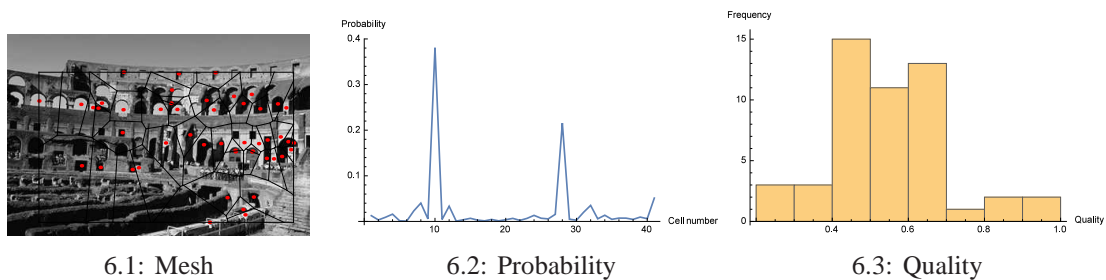
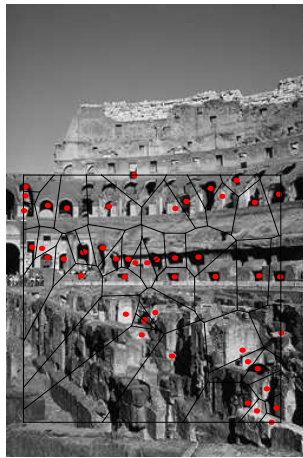


Figure 6. Image Graph Spaces

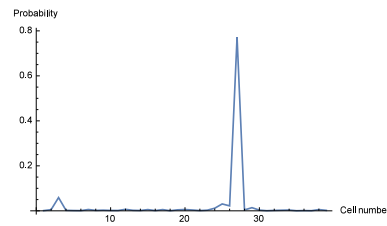
7. Results and Discussion

Most polygons typically have non-zero area so Pr_i is defined for all regions in the plane. In the following image Voronoi graphs, probability functions of cells, image cell qualities and plots of quantities are shown. Also quality of cells and information are studied by examining the nature of the plots. The results of our simulations are shown for only three images per category of the data set given in Fig. 4 for space reasons although the results are presented for the entire data set of 20 images per category amounting to 80 images in total. Corresponding cell area probabilities and distribution of cell qualities are shown next to tessellated spaces in Fig. 5-Fig. 16 in that order.

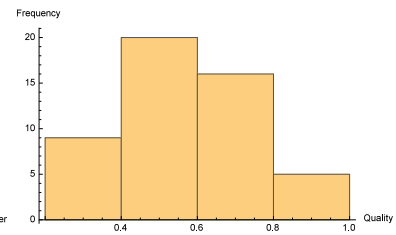
Point patterns consist of a maximum of 50 keypoints and so the resulting cells are usually 50 in number. Notice the nature of the distributions of probabilities and qualities. Probability distri-



7.1: Mesh



7.2: Probability

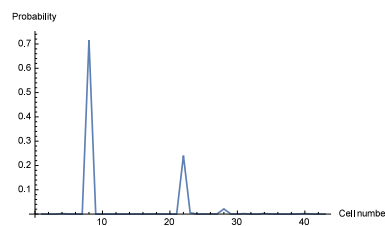


7.3: Quality

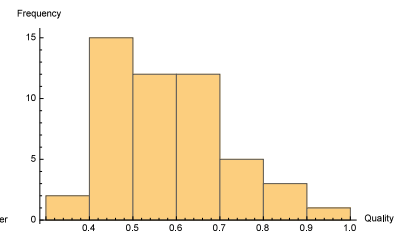
Figure 7. Image Graph Spaces



8.1: Mesh



8.2: Probability



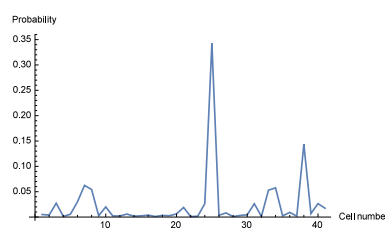
8.3: Quality

Figure 8. Image Graph Spaces

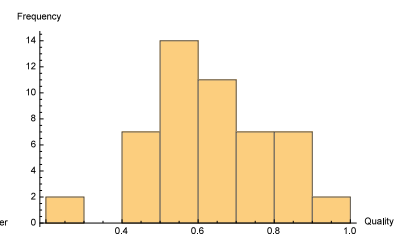
butions range from the extreme of only a few influential cells to cells exhibiting higher tendencies of equal influences. This corresponds to a few large peaks on the probability distributions and a spread out distribution respectively. The qualities of the cells portray the exhibited behaviour.



9.1: Mesh

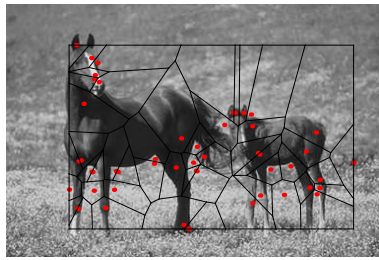


9.2: Probability

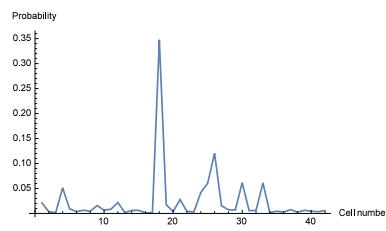


9.3: Quality

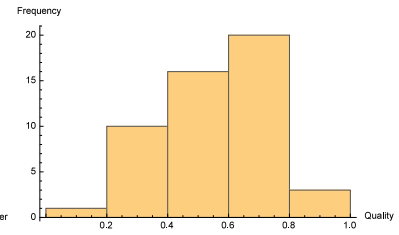
Figure 9. Image Graph Spaces



10.1: Mesh



10.2: Probability

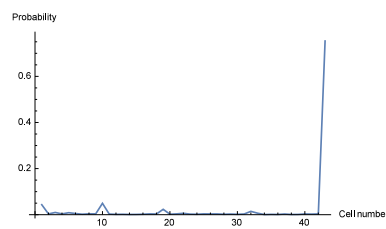


10.3: Quality

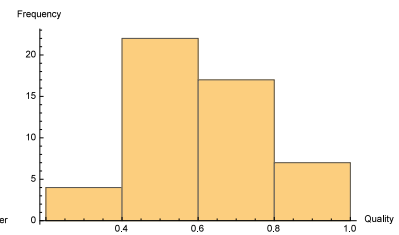
Figure 10. Image Graph Spaces



11.1: Mesh



11.2: Probability

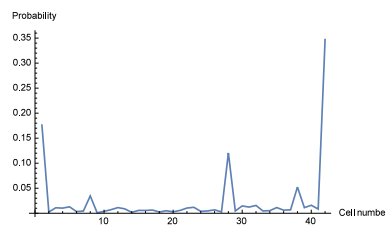


11.3: Quality

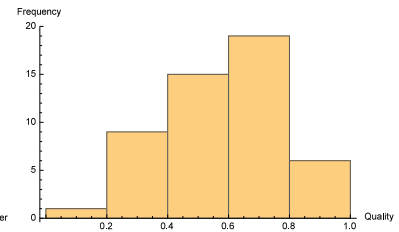
Figure 11. Image Graph Spaces



12.1: Mesh



12.2: Probability



12.3: Quality

Figure 12. Image Graph Spaces

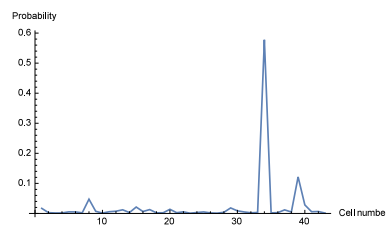
Entropies of tessellations and global quality indices are condensed into the following plots. For 50 Voronoi cells exhibiting a uniform probability distribution the maximum value possible for Renyi entropy is 3.912. All entropy values fall short of this value. Plots of entropies and global qualities are shown for the buildings, horses, humans and mountain scenery categories in Fig. 17. Notice the flat nature of the global qualities for the images. Renyi entropies as a function of the images is non-decreasing.

In the following, plots of global qualities, Renyi entropies and plots of entropies against qualities are shown.

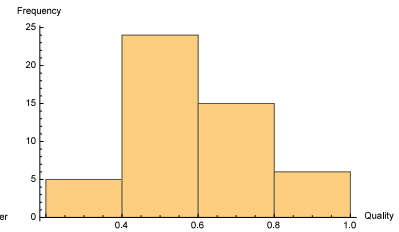
Notice the monotonically increasing entropies and global qualities in Fig. 17. Also observe that



13.1: Mesh

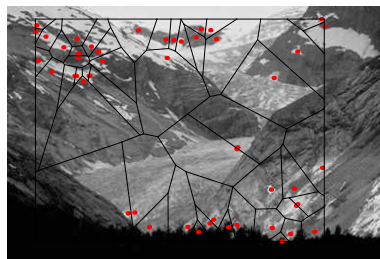


13.2: Probability

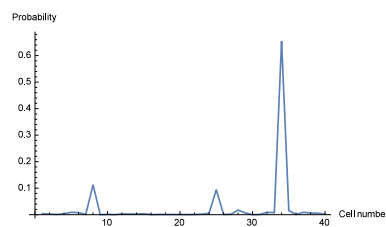


13.3: Quality

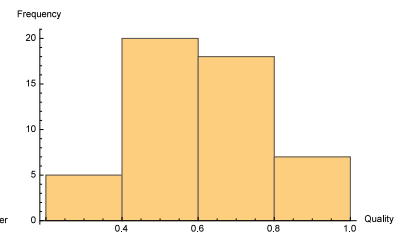
Figure 13. Image Graph Spaces



14.1: Mesh

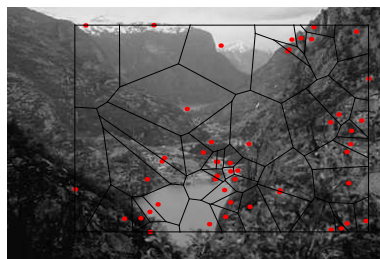


14.2: Probability

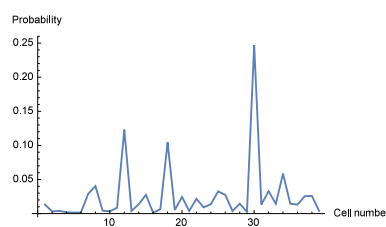


14.3: Quality

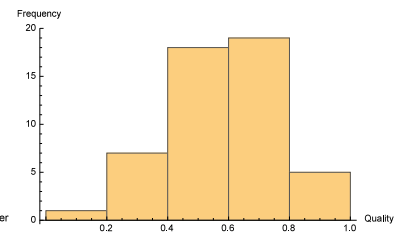
Figure 14. Image Graph Spaces



15.1: Mesh



15.2: Probability



15.3: Quality

Figure 15. Image Graph Spaces

the quantities are distinct across categories. Most importantly entropic information is decreases for $\beta = 1.5, 2.0, 2.5$ in that order. Recall that $\beta = 2$ yields Shannon entropy from the general entropy criterion H . It is interesting to note the oscillating (Fig. 18) as opposed to uniform relationship between entropy and global quality. This confirms the departure of the images from the less interesting case of completely regular patterns.

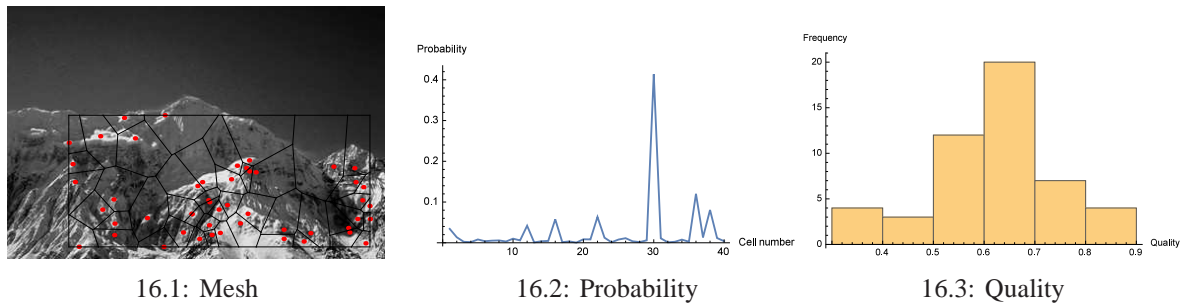


Figure 16. Image Graph Spaces

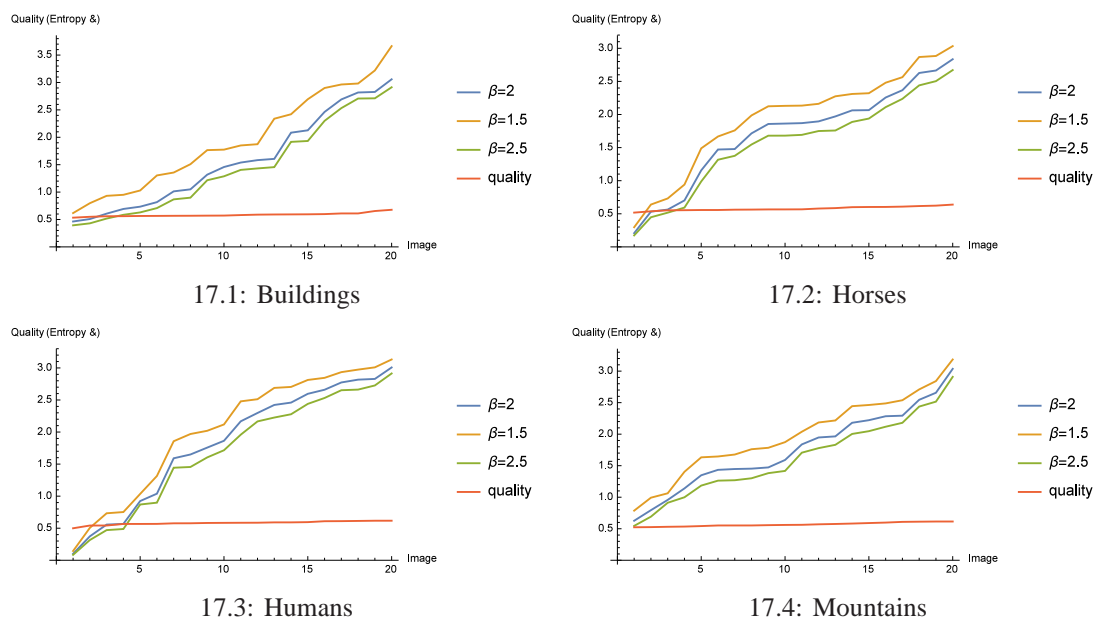


Figure 17. Quantity Relations

8. Conclusion and Future Work

Non-linear probability distribution distribution functions as opposed to uniform ones are observed. However, recall that a uniform distribution maximizes the entropy so that implies that the point patterns are more informative and interesting compared to completely regular patterns. Although the patterns are not uniform the information parameter range of $1 < \beta \leq 2.5$ maximizes the information content of Voronoi cells. This shows that the Renyi entropy is more informative than Shannon entropy. This is due to the variations in pattern structure. Owing to the non-linear relationship between entropy and cell qualities, we see that the patterns are not simple patterns because of the variations.

Notice that the global qualities q_{all} for all image categories practically follow a linear distribution with a gradient close to zero. So given a global quality of a tessellation converging in the

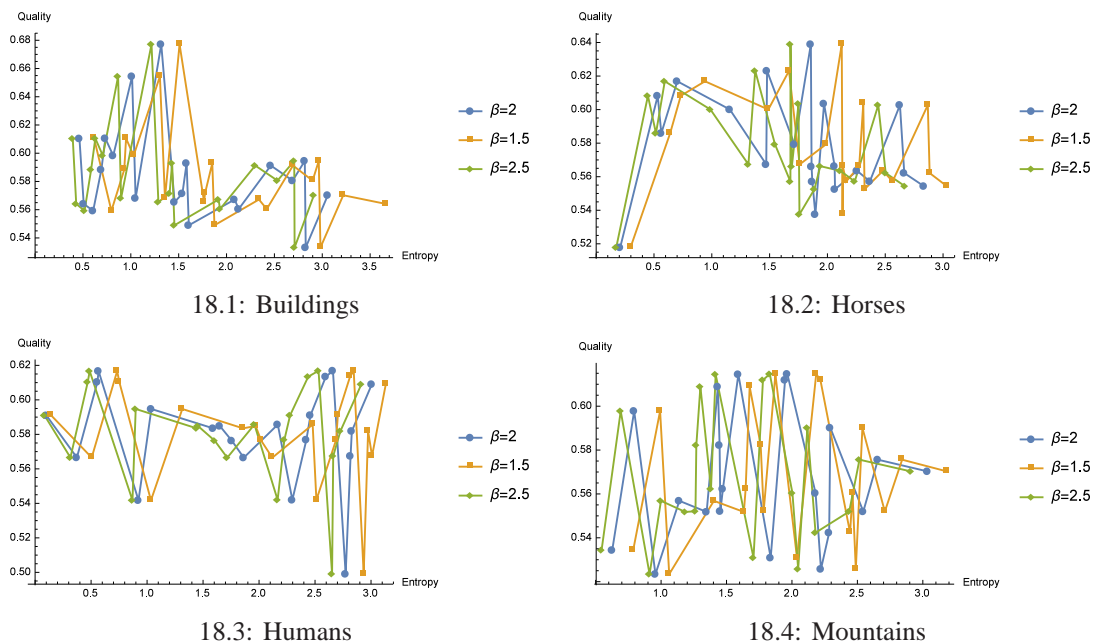


Figure 18. Quality Signatures

neighborhood of $0.5 \leq q_{all} < 1.0$, the point pattern is not completely regular and could be from a digital image. This range of global qualities observed shows that point pattern primitives of digital images may not be simple and completely regular features.

Image point patterns with global quality coefficients in the range $0.5 \leq q_{all} < 1.0$ are stable. This indicates that the image physical system is sufficiently modeled. This is the so called fidelity of solution of the physical system of differential equations represented by the mesh. A completely regular pattern with a global index or fidelity of unity is the most stable (Fig. 3) so that an unstable system has an index of zero or close to zero.

Since the point patterns are not completely regular they contain more information than regular ones because their global indices are less than unity and their entropies are less than the maximum value.

Notwithstanding this quality guarantees for meshes of four or more sides which is hardly studied and much less developed is seen to be stable and guaranteed in the reported range.

Finally it has been shown that the distribution of digital image point patterns is anything but uniform. Therefore future work should reveal the applicable distribution(s).

It goes without saying that although the method is simple and effective in characterizing pattern information and structure the assignment of zero probabilities to infinite Voronoi cells is a disadvantage. This however is a natural consequence of Voronoi partitioning for which the choice has to be made whether the information is attributed to a few infinite cells or otherwise.

References

- A-iyeh, E and JF Peters (2015). Measure of tessellation quality of Voronoï meshes. *Theory and Applications of Mathematics & Computer Science* **5**(2), 158–185.
- Agrell, Erik (1996). Voronoi regions for binary linear block codes. *Information Theory, IEEE Transactions on* **42**(1), 310–316.
- Arbeláez, Pablo A and Laurent D Cohen (2006). A metric approach to vector-valued image segmentation. *International Journal of Computer Vision* **69**(1), 119–126.
- Bern, Marshall and David Eppstein (1995). Mesh generation and optimal triangulation. *Computing in Euclidean geometry* **4**, 47–123.
- Bhatia, RP and KL Lawrence (1990). Two-dimensional finite element mesh generation based on stripwise automatic triangulation. *Computers & Structures* **36**(2), 309–319.
- Bromiley, P.A., N.A. Thacker and E. Bouhova-Thacker (2010). Shannon entropy, Rényi's entropy, and information. Technical report. The University of Manchester, U.K. <http://www.tina-vision.net/docs/memos/2004-004.pdf>.
- Chapman, GP (1970). The application of information theory to the analysis of population distributions in space. *Economic Geography* pp. 317–331.
- Demir, Cigdem and Bülent Yener (2005). Automated cancer diagnosis based on histopathological images: a systematic survey. *Rensselaer Polytechnic Institute, Tech. Rep.*
- Du, Qiang, Vance Faber and Max Gunzburger (1999). Centroidal Voronoi tessellations: applications and algorithms. *SIAM review* **41**(4), 637–676.
- Ebeida, Mohamed S and Scott A Mitchell (2012). Uniform random Voronoi meshes. In: *Proceedings of the 20th International Meshing Roundtable*. pp. 273–290. Springer.
- Goberna, MA, MML Rodríguez and VN Vera de Serio (2012). Voronoi cells via linear inequality systems. *Linear Algebra and Its Applications* **436**(7), 2169–2186.
- Hamanaka, Masatoshi and Keiji Hirata (2002). Applying Voronoi diagrams in the automatic grouping of polyphony. *Information Technology Letters* **1**(1), 101–102.
- Hartley, R.V.L. (1928). Transmission of information. *Bell Systems Technical Journal* p. 535.
- Knupp, Patrick M (2001). Algebraic mesh quality metrics. *SIAM journal on scientific computing* **23**(1), 193–218.
- Leibon, Greg and David Letscher (2000). Delaunay triangulations and voronoi diagrams for riemannian manifolds. In: *Proceedings of the sixteenth annual symposium on Computational geometry*. ACM. pp. 341–349.
- Liu, Jinyi and Shuang Liu (2004). A survey on applications of Voronoi diagrams. *Journal of Engineering Graphics* **22**(2), 125–132.
- McLean, Alex (2007). Voronoi diagrams of music. URL <http://doc.gold.ac.uk/~ma503am/essays/voronoi/voronoi-diagrams-of-music.pdf>. Accessed.
- Mitchell, Scott A (1993). Mesh generation with provable quality bounds. Technical report. Cornell University.
- Møller, Jesper and Øivind Skare (2001). Coloured Voronoi tessellations for Bayesian image analysis and reservoir modelling. *Statistical modelling* **1**(3), 213–232.
- Nyquist, H. (1924). Certain factors affecting telegraph speed. *Bell Systems Technical Journal* p. 324.
- Owen, Steven J (1998). A survey of unstructured mesh generation technology. In: *IMR*. pp. 239–267.
- Persson, Per-Olof (2004). Mesh generation for implicit geometries. PhD thesis. Citeseer.
- Persson, Per-Olof and Gilbert Strang (2004). A simple mesh generator in matlab. *SIAM review* **46**(2), 329–345.
- Peters, James F (2016). Computational Proximity. Excursions in the Topology of Digital Images. *Intelligent Systems Reference Library*. viii + 445pp., DOI:10.1007/978-3-319-30262-1, in press.
- Peters, J.F. (2015a). Proximal delaunay triangulation regions. *PJMS [Proc. of the Korean Math. Soc.]*. to appear.

- Peters, J.F. (2015b). Proximal Voronoï regions, convex polygons, & Leader uniform topology. *Advances in Math.* **4**(1), 1–5.
- Peters, J.F. (2015c). Visibility in proximal Delaunay meshes. *Advances in Math.* to appear.
- Ramella, Massimo, Mario Nonino, Walter Boschini and Dario Fadda (1998). Cluster identification via voronoi tessellation. *arXiv preprint astro-ph/9810124*.
- Rao, C Radhakrishna (1982). Diversity and dissimilarity coefficients: a unified approach. *Theoretical population biology* **21**(1), 24–43.
- Rényi, A. (2011). On measures of entropy and information. In: *Proceedings of the 4th Berkeley Symposium on Math., Statist. and Probability*. University of California Press, Berkeley, Calif.. pp. 547–547. vol. 1, Math. Sci. Net. Review MR0132570.
- Shewchuk, J (2002). What is a good linear finite element? interpolation, conditioning, anisotropy, and quality measures (preprint). *University of California at Berkeley*.
- Voronoi, G. (1903). Sur un problème du calcul des fonctions asymptotiques. *J. für die reine und angewandte Math.* **126**, 241–282. JFM 38.0261.01.
- Voronoi, G. (1907). Nouvelles applications des paramètres continus à la théorie des formes quadratiques. premier mémoire. *J. für die reine und angewandte Math.* **133**, 97–178.
- Voronoi, G. (1908). Sur un problème du calcul des fonctions asymptotiques. *J. für die reine und angewandte Math.* **134**, 198–287. JFM 39.0274.01.
- Wang, James Ze, Jia Li and Gio Wiederhold (2001). Simplicity: Semantics-sensitive integrated matching for picture libraries. *Pattern Analysis and Machine Intelligence, IEEE Transactions on* **23**(9), 947–963.
- Xu, Dongxin and Deniz Erdogmus (2010). Renyi’s entropy, divergence and their nonparametric estimators. In: *Information Theoretic Learning*. pp. 47–102. Springer.
- Zhou, Rongxi, Ru Cai and Guanqun Tong (2013). Applications of entropy in finance: A review. *Entropy* **15**(11), 4909–4931.